2015-02

Correction of Depth Bias in Upper-Ocean Temperature and Salinity Profiling Measurements from Airborne Expendable Probes

SPECIAL
DYNAMO/CINDY/AMIE/LASP
COLLECTION

Correction of Depth Bias in Upper-Ocean Temperature and Salinity Profiling Measurements from Airborne Expendable Probes

DENNY P. ALAPPATTU AND QING WANG

Department of Meteorology, Naval Postgraduate School, Monterey, California

(Manuscript received 16 June 2014, in final form 21 October 2014)

ABSTRACT

During the Dynamics of Madden–Julian Oscillation (DYNAMO) Experiment in 2011, airborne expendable conductivity–temperature–depth (AXCTD) probes and airborne expendable bathythermographs (AXBTs) were deployed using NOAA's WP-3D Orion aircraft over the southern tropical Indian Ocean. From initial analysis of the AXCTD data, about 95% of profiles exhibit double mixed layer structures. The presence of a mixed layer from some of these profiles were erroneous and were introduced because of the AXCTD processing software not being able to correctly identify the starting point of the probe descent. This work reveals the impact of these errors in data processing and presents an objective method to remove such erroneous data from the profiles using spectrograms from raw audio files. Reconstructed AXCTD/AXBT profiles are compared with collocated shipborne conductivity–temperature–depth (CTD) and expendable bathythermograph (XBT) profiles and are found to be in good agreement.

1. Introduction

For decades, airborne expendable bathythermographs (AXBTs) have been used extensively for sampling ocean temperature profiles for oceanic surveys and research (e.g., Bane and Sessions 1984; Dinegar Boyd 1987; Watts et al. 1989; Price et al. 1994; Rodríguez-Santana et al. 1999). Recently, airborne expendable conductivity–temperature–depth (AXCTD) probes were developed to obtain both temperature and salinity profiles (Chu and Fan 2001; Shay and Brewster 2010). These air-deployable expendable probes are easily deployable and relatively inexpensive. Their broad applications to the research and operation communities are hence not surprising.

AXCTD/AXBT probes measure the ocean temperature and salinity similarly to their shipborne counterparts, expendable conductivity–temperature–depths (XCTDs) and expendable bathythermographs (XBTs) (e.g.: Yabuki et al. 2006; Levitus et al. 2009; Stephenson et al. 2012). Airborne measurements provide several advantages over those made by XCTDs/XBTs. With the high mobility of an aircraft, AXBT/AXCTD can sample a relatively large area within a short time period, providing spatial variability of the upper ocean down to 1000-m depth with vertical resolutions of less than 1 m. They can be deployed over treacherous oceanic regions and under severe weather conditions like hurricanes, impassable for ships (e.g.: Uhlhorn and Shay 2012); measurements from these probes are made in undisturbed near-surface waters, which contrast with shipboard measurements. AXCTD/AXBT measurements, in conjunction with dropsonde data, can provide a three-dimensional depiction of atmospheric and oceanographic thermal structures and important variables in air–sea coupling at near-surface levels (Bane et al. 2004). Accurate measurements in the upper few meters of ocean are imperative for air–sea interaction applications.

Understanding air–sea interaction on the Madden–Julian oscillation (MJO) time scale is a major objective of the Dynamics of MJO (DYNAMO; October 2011–March 2012) conducted over the central tropical Indian Ocean (Yoneyama et al. 2013). During DYNAMO, 114 AXCTDs and 321 AXBTs were deployed in 12 research flights between 11 November and 13 December 2011 using NOAA's WP-3D Orion aircraft (P-3) in the southern tropical Indian Ocean. The 12 flights of the P-3 during DYNAMO were made in three phases of the

Corresponding author address: Denny P. Alappattu, Department of Meteorology, Naval Postgraduate School, 589 Dyer Road, Root Hall, Monterey, CA 93943-5114.
E-mail: dpalappa@nps.edu

DOI: 10.1175/JTECH-D-14-00114.1

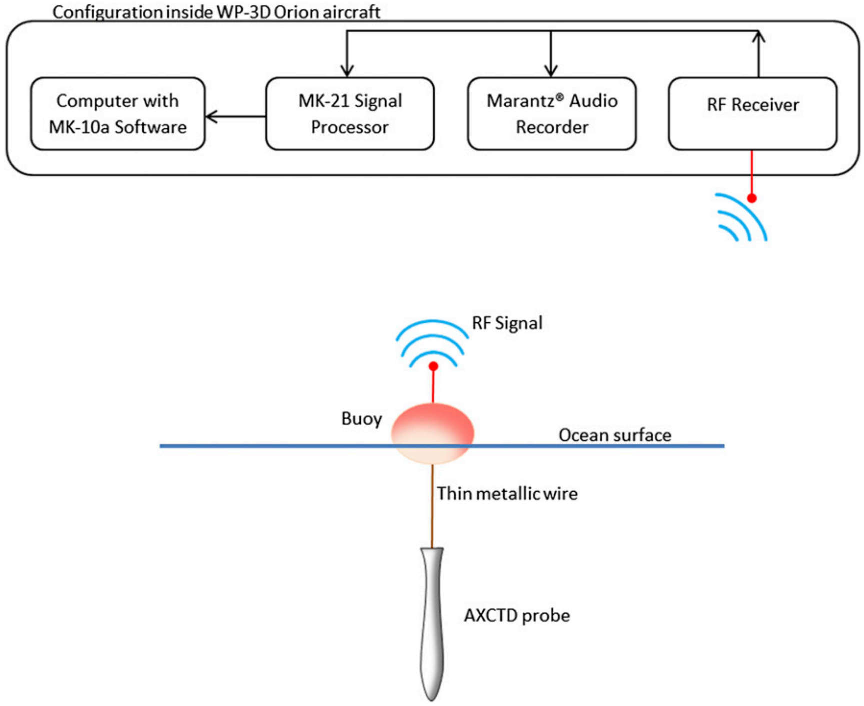

FIG. 1. Block diagram of various components of the AXCTD/AXBT probe and data acquisition system.

MJO event over the southern tropical Indian Ocean in November 2011. The purposes of this research note are to document AXCTD/AXBT data quality issues and introduce a method to remove the depth biases in AXCTD profiles using spectrograms from the AXCTD probes' raw audio files.

2. Data and methods

a. AXBT/AXCTD deployment

Deployment procedures of the AXCTD/AXBT probes during DYNAMO are briefly described in this section. During DYNAMO, the P-3 deployed AXBT/AXCTD probes from various altitudes. While AXCTD probes can be deployed only from the internal chute, the AXBT probes can be deployed internally and externally. Figure 1 summarizes the AXCTD/AXBT transmission, receiving, and data processing systems on the P-3. AXCTD/AXBT probes launched from the aircraft are slowed down with a small parachute to reduce the impact speed at the ocean surface. Upon impact, a small buoy inflates to host the radio transmitter. Seawater activates the battery and turns on the transmitter at three frequencies (channels 12, 14, and 16 at 170, 171.5, and 173 MHz, respectively). After establishing communication with the aircraft-based radio frequency (RF) receiver, the probe is released from its canister and descends through the water column. The probe sends measurements to its surface unit inside the buoy, connected by a thin copper wire, and the surface unit transmits data to the aircraft-based RF receiver. On the aircraft side, a Marantz PMD 560 recorder digitizes analog signals from the aircraft RF receiver into an audio (.wav) file onto a compact flash card. Simultaneously, a Sippican MK21 Oceanographic Data Acquisition System processes the data in real time using Sippican MK10a signal processing software. Raw profiles are displayed at the AXBT/AXCTD processing console in near–real time for initial data assessment. After initial data processing, an ASCII log file (.dta) is created for AXBT and AXCTD data.

b Depth information and bias in expendable probes

Similar to the XBTs/XCTDs, the AXBT/AXCTD probes also do not carry pressure sensors; therefore, depth is estimated using a fall rate equation (FRE) from the time elapsed after the probe is released from the canister. Using FRE, depth (d) at elapsed time (t) is calculated as

$$d(t) = at + bt^2, \quad (1)$$

where a and b are fall rate equation coefficients (FREC), provided by the manufacturer (Hanawa et al. 1995; DiNezio and Goni 2010; Hutchinson et al. 2013). Several studies have shown that, XBT/XCTD temperature measurements show a systematic increase of 0.1°–0.2°C

(Fierl and Robinson 1977; Seaver and Kuleshov 1982). Later on, Gouretski and Koltermann (2007) discovered a time-varying positive temperature bias in the XBT database. Since the XBT data are the largest proportion of the dataset, this bias resulted in a significant increase in the global ocean heat content (GOHC) trend from the 1950s to the present (Gouretski and Koltermann 2007). XCTD measurements were also not free from the bias (Kizu et al. 2008; Boyer et al. 2011). The fall rate of expendable probes varies with water mass properties (Boyer et al. 2011; Thadathil et al. 2002), type of the probe (Kizu et al. 2008), and depth (Levitus et al. 2009), and there is evidence that the fall rate has changed over time (Cowley et al. 2013; DiNezio and Goni 2011; Gouretski 2012, Hamon et al. 2012; Levitus et al. 2009). By now it is well established that the temperature bias in the expendable probes arises from 1) depth bias caused by the under- or overcalculation of depth when using the manufacturer-provided FREC (Johnson 1995; Hanawa et al. 1995; Kizu et al. 2005, 2008, 2011; DiNezio and Goni 2010; Boyer et al. 2011; Hutchinson et al. 2013; Goes et al. 2013; Cowley et al. 2013; Cheng et al. 2014); and 2) pure temperature bias, independent of FREC originating from the thermistor errors or introduced by data acquisition system (Reseghetti et al. 2007; Gouretski and Reseghetti 2010; Cowley et al. 2013; Cheng et al. 2014). The depth bias can be separated from the pure temperature bias (DiNezio and Goni 2011; Gouretski and Reseghetti 2010). A widely accepted method to correct these biases is comparing the XBT/AXCTD profiles with the contemporaneous CTD profiles and modifying the manufacturer-provided FREC (Hanawa et al. 1995; Kizu et al. 2008, Gouretski and Reseghetti 2010; Cowley et al. 2013; Cheng et al. 2014). Recently, Cowley et al. (2013) and Cheng et al. (2014) characterized and separated out pure temperature bias from depth error using more than 4000 XBT–CTD side-by-side pairs and global XBT–CTD pairs. Their research has presented promising results to correct the historical XBT database.

Even with perfect FREC, depth bias occurs in AXCTD data due to the inaccurate detection of the start time of the probe descent, which is the issue to be discussed in this paper. The problem is related to the false detection of elapsed time before the probe is released from the surface unit. An objective method for postdeployment correction is described in this paper. In this study we use the Johnson (1995) proposed revised FREC ($a = 3.227$ and $b = -2.17 \times 10^{-4}$) to retrieve depth information.

3. Depth bias in AXCTD measurements

Initial examination of the DYNAMO data revealed about 95% of AXCTD profiles showing a distinctive two-layered structure in the upper ocean, especially in the salinity profile. Figure 2 gives an example of this two-layered structure using the original AXCTD temperature (red solid line) and salinity (blue solid line) profiles taken at 0714 UTC 26 November 2011 (at 0.30°N, 80.47°E). Here, the large vertical gradients in temperature and salinity at approximately 100 m identify the bottom of the mixed layer. However, there exists an apparent fresher water layer at the top down to 30.6 m below the surface. In this particular example, the temperature profile does not indicate similar layering in the top level, although many other profiles also have layering signature in temperature. The apparent upper mixed layer with less saline water varied between several meters to 35 m in depth, with the majority being around ~30 m. This top mixed layer was found to be an artifact of the processing software not being able to correctly detect the starting time of the probe descent. It is a result of starting the depth

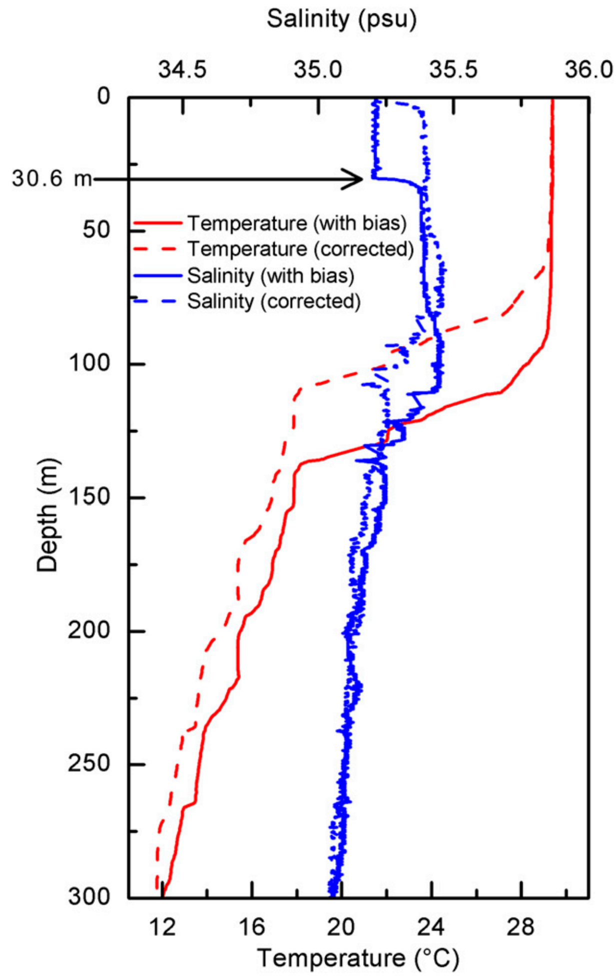

FIG. 2. Example of AXCTD temperature and salinity profiles with depth bias and profiles corrected for depth bias.

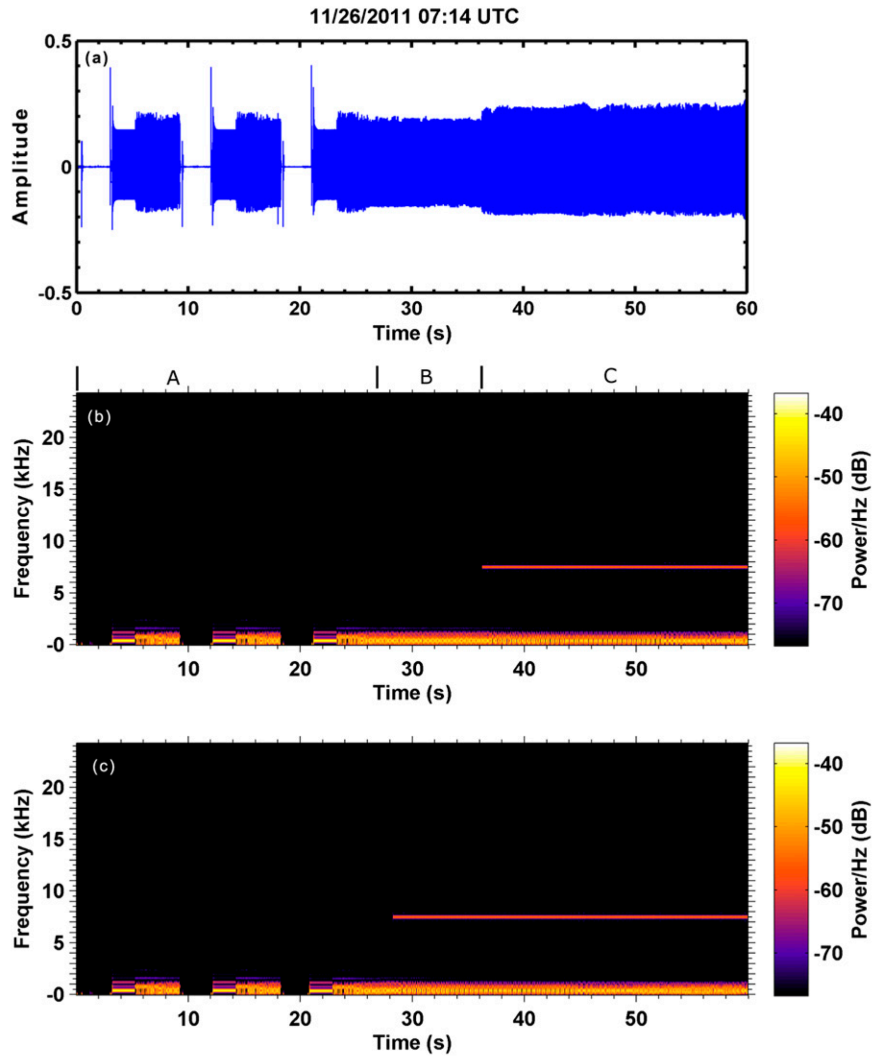

FIG. 3. (a) Waveform and (b) spectrogram of audio signal having erroneous data corresponding to depth bias. (c) Spectrogram of audio signal after removing the erroneous signal.

calculation when the probe was actually sitting at the surface. Applying the values for a and b in Eq. (1), it can be estimated that a depth bias of 30.6 m corresponds to false detection of the starting time of descent by about 9.5 s.

Depth biases in the AXCTD profiles are a known issue to the AXCTD manufacturer, Lockheed Martin Sippican. A general practice is to manually remove the top layer based on visual inspection (G. Johnson, Lockheed Martin Sippican, 2012, personal communication). An independent system, the MK150 processing system by Tsurumi Seiki Company also failed to consistently correct the depth error. Such depth bias does not exist in the processed AXBT profiles.

This depth bias in the AXCTD measurements produces misleading results, especially when the ocean measurements come from a mixture of both AXBT and AXCTD probes. An important step in quality control of the AXCTD data is thus to remove the bias using an objective and consistent method, which is the focus of this work. In addition, since AXBT and AXCTD data are used together, a comparison of the temperature

TABLE 1. Statistics of depth bias estimated using the spectrogram method.

No. of profiles (n)	Mean (m)	Median (m)	Std dev (m)	Min (m)	Max (m)
103	30.13	30.70	2.59	19.80	38.00

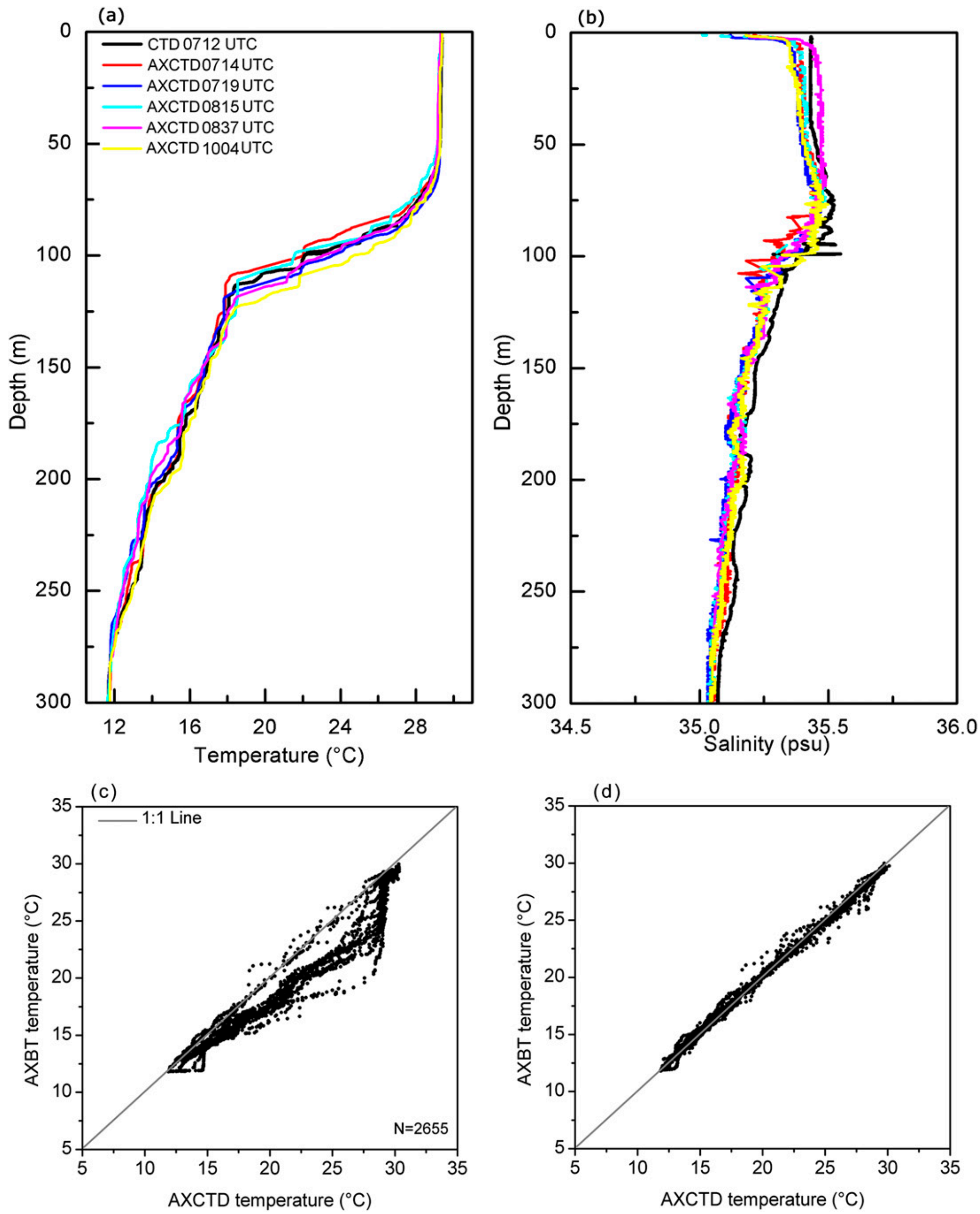

FIG. 4. Comparison of AXCTD (a) temperature and (b) salinity profiles with collocated CTD measurements from R/V *Revelle*. (c) Scatterplot between collocated AXCTD temperature measurements with depth bias and AXBT temperature measurements. (d) As in (c), but for AXCTD temperature measurements corrected for depth bias.

measurements from both probes are given to identify any potential bias between the sensors.

4. Depth bias correction

This section describes a method to correct depth bias in the AXCTD measurements based on the spectrogram of AXCTD audio data. The signal transmitted to the airplane from the float has two components: one from the probe with the measured data and the other a ''launch'' tone at 7.5 kHz that is added by the electronics in the buoy and mixed with the probe signal prior to transmission to the airplane. The launch tone is used to indicate when the probe has been released from the float. This tone was designed to be detected by the MK21 signal processor, which communicates the information to the

MK10a software. The depth bias and the no-depth issues are related to MK21 detecting the launch tone too early or not detecting the tone at all. Based on our discussion with the manufacturer (G. Johnson, Lockheed Martin Sippican, 2013, personal communication), these issues can be alleviated by adjusting the launch tone signal strength in the MK21 processor setting and reprocessing the audio data. Instead of a trial and error manual process, we present an automated and objective method here using the spectrogram of the audio signal described below.

Figure 3a shows the first minute of raw audio data in wave form; Fig. 3b shows the corresponding spectrogram of the same data. For simplicity of discussion, regions A–C divide the signal into three segments. In region A, there are three sections of audio data separated by about 3 s without signal. Each section contains 2 s of synchronization frames followed by 4 s of calibration data, and all three sections have the same length. After the third replica of synchronized/calibrated frames (at 27 s), the sensor data were received. The beginning of region B can be identified in this manner. However, the probe descent does not start until the launch tone appears. The signal in region B is mistaken as part of the profile if the descending elapsed time started at the beginning of region B. This results in the apparent "well mixed layer" seen in the erroneous temperature and salinity profiles. In the example in Fig. 3b, region B starts immediately after the third synchronization and calibration signal and lasts about 9.5 s, which corresponds to the observed depth bias (30.6 m) in the temperature and salinity profiles. Region C corresponds to the actual temperature and salinity data signal during the descent. The spectrogram (Fig. 3b) clearly shows that the two signals are superimposed on each other, one is the temperature and salinity data at low frequencies and the other is the 7.5-kHz launch tone. This spectral characteristic is used to identify the end of region B. The erroneous region (B) is then removed from all AXCTD audio data. Figure 3c shows the spectrogram of the corrected audio signal. The average depth bias estimated using the spectrogram method was 30.14 ± 0.25 m. The statistics of the observed depth bias is given in Table 1. AXCTD data were reprocessed using the MK21 system with MK10a processing software to produce profiles corrected for depth bias. The dashed lines in Fig. 2 show corrected temperature (red) and salinity (blue) profiles.

5. Evaluation of depth-bias-corrected AXCTD data

The AXCTD depth-bias-corrected profiles were compared with collocated CTD casting made from the R/V *Roger Revelle* at 0712 UTC on the same day. Figure 4a shows the depth-bias-corrected AXCTD temperature profile (red curve) in better agreement with the CTD profile (black curve). Other depth-bias-corrected AXCTD temperature profiles taken within the ~3-h and ~50-km range of the CTD casting are consistent with the CTD measurements in terms of mixed layer structure. Figure 4b shows AXCTD salinity profiles, which also match well with the CTD profiles. AXBT measurements also show good agreement with R/V *Revelle* CTD temperature data (not shown).

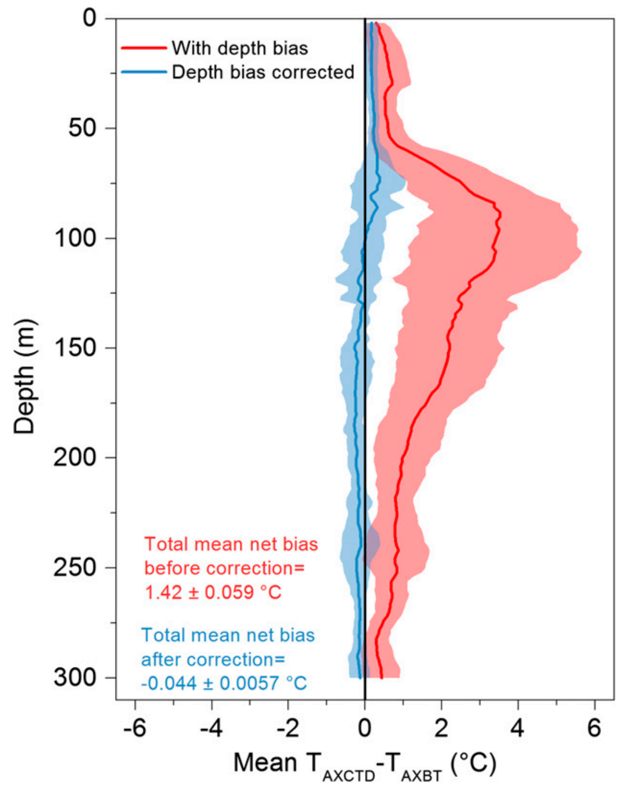

FIG. 5. Profiles of mean and standard deviation of AXCTD and AXBT temperature difference with and without depth bias correction.

For further evaluation of depth-bias-corrected temperature profiles, 20 AXCTD–AXBT pairs were analyzed. Each pair was within a time difference of 2 min from each other and separated by a distance of less than 70 km. Figure 4c shows the comparison of temperatures of AXCTDs with depth bias and corresponding collocated AXBTs. Temperatures between the surface and 300 m are only considered here for comparison. Data points lie scattered away from the 1:1 line, showing that AXCTD temperature profiles without depth correction are consistently higher than AXBT temperatures. Figure 4d shows the temperature scatterplot of AXCTD–AXBT pairs using the depth-bias-corrected AXCTD profiles.

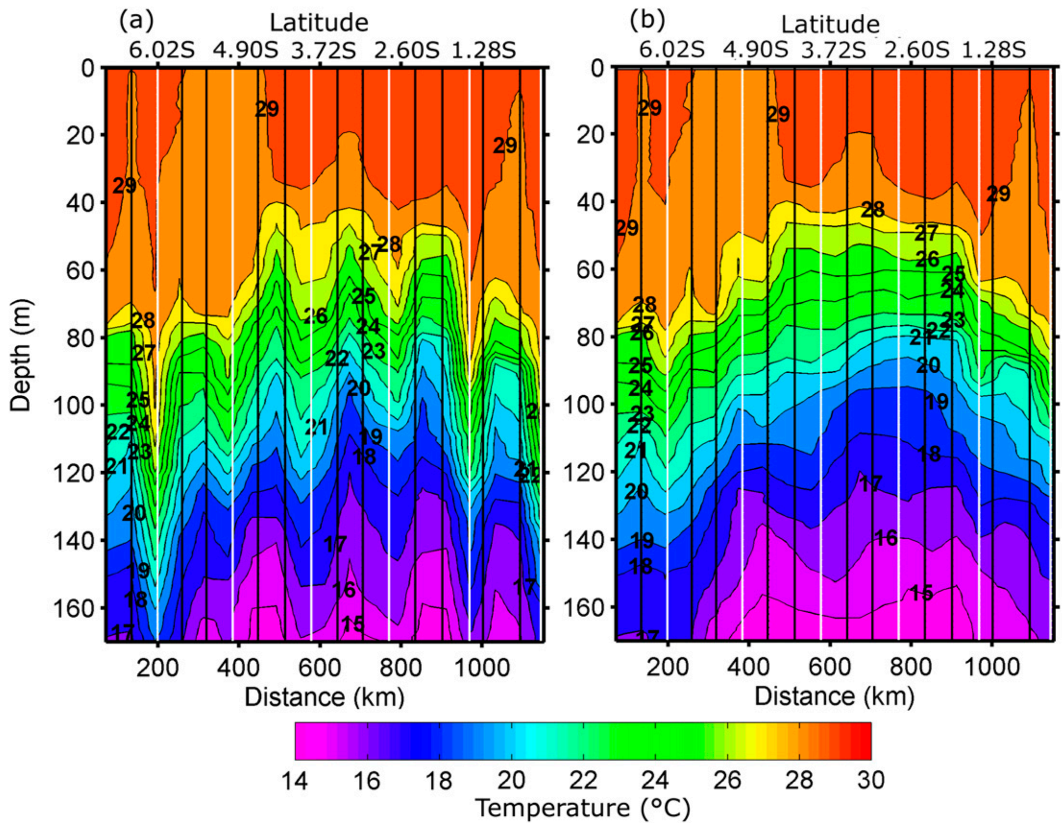

FIG. 6. Vertical cross section of temperature along the diagonal transect from Diego Garcia to R/V *Revelle* (a) using profiles from AXBTs and AXCTDs without depth bias correction and (b) using the same profiles corrected for depth bias. Positions of AXBT and AXCTD drops relative to Diego Garcia are shown by black and white lines, respectively.

Depth bias corrections removed the large scatter observed in Fig. 4c and data points fall close to the 1:1 line. Profiles of mean temperature difference between the AXCTD–AXBT pairs are shown in Fig. 5; shading represents one standard deviation. Temperature differences between AXCTD and AXBT peak around 100-m depth when using uncorrected depth-biased AXCTD profiles (red). Mean AXCTD–AXBT temperature differences are low at all depths after correcting for depth biases in AXCTD temperature profiles (blue). Depth bias correction reduced the total mean temperature bias considerably from 1.42° ± 0.059°C to −0.044° ± 0.00057°C.

Depth biases in the AXCTD profiles can lead to the wrong interpretation of the observations. Figure 6a shows the vertical cross section of temperature from the AXBTs and uncorrected AXCTD profiles taken along the diagonal transect from Diego Garcia (7.3117°S, 72.4167°E) to the R/V *Revelle* stationed at 0.0217°N, 80.5012°E. Distances from Diego Garcia are shown in the lower *x* axis and corresponding latitudes are in the upper *x* axis. The positions of AXBT and AXCTD drops relative to Diego Garcia are shown by black and white lines, respectively. The vertical cross section of temperature shows a wavelike structure in the thermocline. Figure 6b shows the same temperature cross-section measurements using the depth-bias-corrected AXCTD profiles. Depth bias correction removed the erroneous wavy structures in the thermocline region, and the presence of the Seychelles–Chagos thermocline ridge (SCTR) in the southern Indian Ocean is clearly seen in the resultant figure. These results provide the confidence that the spectrogram method effectively removes the depth bias from the AXCTD profiles.

6. Summary

Accurate measurements in the upper few meters of the ocean are essential to estimate air–sea heat fluxes and ocean heat content. However, measurements from the air-deployable expendable bathythermograph probes, especially the AXCTD probes, may result in erroneous profiles because of data processing software not detecting the correct probe descend time for some launch tone strength settings. The work presented here provides an objective and automated method to detect and correct the depth bias.

AXCTD and AXBT probes were deployed in the central tropical Indian Ocean during the Dynamics of Madden–Julian Oscillation (DYNAMO) field experiment to collect accurate high-resolution measurements of upper-ocean temperature and salinity. AXCTD profiles exhibited the presence of an artificial shallow mixed layer at the top of the water extending to as far as 35 m below the surface. Removing the depth bias in individual profiles manually was subject to inconsistencies and human errors. Here we used an alternative approach through the analysis of a spectrogram of audio files. This method objectively removed the section that causes errors in identifying the start of the launch tone in the data processing software. Quality and consistency of these data corrected for depth biases are proved by comparisons with the independent CTD and simultaneous AXBT measurements. This method is suitable for screening the AXCTD profiles for depth biases as well as further improving the AXCTD data processing system.

Acknowledgments. This work was supported by ONR Award N0001413WX20025 and partly by NSF Award AGS1062300. Denny P. Alappattu is sponsored by the National Research Council research associateship program. Discussions and input from Grant Johnson and Peter Black were very helpful. The hard work of Lt. David Tramp, LCDR Heather Hornick Quilenderino, and LCDR Robin Corey Cherrett in data collection and processing are greatly appreciated. Dr. James Moum of Oregon State University provided the CTD cast data from R/V *Revelle*.

REFERENCES

Bane, J. M., Jr., and M. H. Sessions, 1984: A field performance test of the Sippican deep aircraft-deployed expendable bathythermograph. *J. Geophys. Res.,* **89,** 3615–3621, doi:10.1029/JC089iC03p03615.

——, R. Bluth, C. Flagg, C. A. Friehe, H. Jonsson, W. K. Melville, M. Prince, and D. Riemer, 2004: UNOLS establishes SCOAR to promote research aircraft facilities for U.S. ocean sciences. *Oceanography,* **17,** 176–185, doi:10.5670/oceanog.2004.14.

Boyer, T., and Coauthors, 2011: Investigation of XBT and XCTD bias in the Arabian Sea and the Bay of Bengal with implications for climate studies. *J. Atmos. Oceanic Technol.,* **28,** 266–286, doi:10.1175/2010JTECHO784.1.

Cheng, L., J. Zhu, R. Cowley, T. Boyer, and S. Wijffels, 2014: Time, probe type, and temperature variable bias corrections to historical expendable bathythermograph observations. *J. Atmos. Oceanic Technol.,* **31,** 1793–1825, doi:10.1175/JTECH-D-13-00197.1.

Chu, P. C., and C. Fan, 2001: Low salinity, cool-core cyclonic eddy detected northwest of Luzon during the South China Sea Monsoon Experiment (SCSMEX) in July 1998. *J. Oceanogr.,* **57,** 549–563, doi:10.1023/A:1021251519067.

Cowley, R., S. Wijffels, L. Cheng, T. Boyer, and S. Kizu, 2013: Biases in expendable bathythermograph data: A new view based on historical side-by-side comparisons. *J. Atmos. Oceanic Technol.,* **30,** 1195–1225, doi:10.1175/JTECH-D-12-00127.1.

Dinegar Boyd, J. D., 1987: Improved depth and temperature conversion equations for Sippican AXBTs. *J. Atmos. Oceanic Technol.,* **4,** 545–551, doi:10.1175/1520-0426(1987)004<0545:IDATCE>2.0.CO;2.

DiNezio, P. N., and G. J. Goni, 2010: Identifying and estimating biases between XBT and Argo observations using satellite altimetry. *J. Atmos. Oceanic Technol.,* **27,** 226–240, doi:10.1175/2009JTECHO711.1.

——, and ——, 2011: Direct evidence of a changing fall-rate bias in XBTs manufactured during 1986–2008. *J. Atmos. Oceanic Technol.,* **28,** 1569–1578, doi:10.1175/JTECH-D-11-00017.1.

Flierl, G. R., and A. R. Robinson, 1977: XBT measurements of thermal gradients in the MODE eddy. *J. Phys. Oceanogr.,* **7,** 300–302, doi:10.1175/1520-0485(1977)007<0300:XMOTGI>2.0.CO;2.

Goes, M., G. Goni, and K. Keller, 2013: Reducing biases in XBT measurements by including discrete information from pressure switches. *J. Atmos. Oceanic Technol.,* **30,** 810–824, doi:10.1175/JTECH-D-12-00126.1.

Gouretski, V., 2012: Using GEBCO digital bathymetry to infer depth biases in the XBT data. *Deep-Sea Res. I,* **62,** 40–52, doi:10.1016/j.dsr.2011.12.012.

——, and K. P. Koltermann, 2007: How much is the ocean really warming? *Geophys. Res. Lett.,* **34,** L01610, doi:10.1029/2006GL027834.

——, and F. Reseghetti, 2010: On depth and temperature biases in bathythermograph data: Development of a new correction scheme based on analysis of a global ocean database. *Deep-Sea Res. I,* **57,** 812–833, doi:10.1016/j.dsr.2010.03.011.

Hamon, M., G. Reverdin, and P.-Y. Le Traon, 2012: Empirical correction of XBT data. *J. Atmos. Oceanic Technol.,* **29,** 960–973, doi:10.1175/JTECH-D-11-00129.1.

Hanawa, K., P. Rual, R. Bailey, A. Sy, and M. Szabados, 1995: A new depth-time equation for Sippican or TSK *T-7, T-6,* and *T-4* expendable bathythermographs (XBT). *Deep-Sea Res. I,* **42,** 1423–1451, doi:10.1016/0967-0637(95)97154-Z.

Hutchinson, K. A., S. Swart, I. J. Ansorge, and G. J. Goni, 2013: Exposing XBT bias in the Atlantic sector of the Southern Ocean. *Deep-Sea Res. I,* **80,** 11–22, doi:10.1016/j.dsr.2013.06.001.

Johnson, G. C., 1995: Revised XCTD fall-rate equation coefficients from CTD data. *J. Atmos. Oceanic Technol.,* **12,** 1367–1373, doi:10.1175/1520-0426(1995)012<1367:RXFREC>2.0.CO;2.

Kizu, S., S. Ito, and T. Watanabe, 2005: Inter-manufacturer difference and temperature dependency of the fall rate of T-5 expendable bathythermograph. *J. Oceanogr.,* **61,** 905–912, doi:10.1007/s10872-006-0008-z.

——, H. Onishi, T. Suga, K. Hanawa, T. Watanabe, and H. Iwamiya, 2008: Evaluation of the fall rates of the present and developmental XCTDs. *Deep-Sea Res. I,* **55,** 571–586, doi:10.1016/j.dsr.2007.12.011.

——, C. Sukigara, and K. Hanawa, 2011: Comparison of the fall rate and structure of recent T-7 XBT manufactured by Sippican and TSK. *Ocean Sci.,* **7,** 231–244, doi:10.5194/os-7-231-2011.

Levitus, S., J. I. Antonov, T. P. Boyer, R. A. Locarnini, H. E. Garcia, and A. V. Mishonov, 2009: Global ocean heat content 1955–2008 in light of recently revealed instrumentation problems. *Geophys. Res. Lett.,* **36,** L07608, doi:10.1029/2008GL037155.

Price, J. M., M. L. Van Woert, and M. Vitousek, 1994: On the possibility of a ridge current along the Hawaiian Islands. *J. Geophys. Res.,* **99,** 14 101–14 111, doi:10.1029/94JC00838.

Reseghetti, F., M. Borghini, and G. M. R. Manzella, 2007: Factors affecting the quality of XBT data—Results of analyses on profiles from the western Mediterranean Sea. *Ocean Sci.,* **3,** 59–75, doi:10.5194/os-3-59-2007.

Rodríguez-Santana, A., J. L. Pelegrí, P. Sangrà, and A. Marrero-Díaz, 1999: Diapycnal mixing in Gulf Stream meanders. *J. Geophys. Res.,* **104,** 25 891–25 912, doi:10.1029/1999JC900219.

Seaver, G. A., and S. Kuleshov, 1982: Experimental and analytical error of the expendable bathythermograph. *J. Phys. Oceanogr.,* **12,** 592–600, doi:10.1175/1520-0485(1982)012<0592:EAAEOT>2.0.CO;2.

Shay, L. K., and J. K. Brewster, 2010: Eastern Pacific oceanic heat content estimation for hurricane intensity forecasting. *Mon. Wea. Rev.,* **138,** 2110–2131, doi:10.1175/2010MWR3189.1.

Stephenson, G. R., Jr., S. T. Gille, and J. Sprintall, 2012: Seasonal variability of upper ocean heat content in Drake Passage. *J. Geophys. Res.,* **117,** C04019, doi:10.1029/2011JC007772.

Thadathil, P., A. K. Saran, V. V. Gopalakrishna, P. Vethamony, N. Araligidad, and R. Bailey, 2002: XBT fall rate in waters of extreme temperature: A case study in the Antarctic Ocean. *J. Atmos. Oceanic Technol.,* **19,** 391–396, doi:10.1175/1520-0426-19.3.391.

Uhlhorn, E. W, and L. K. Shay, 2012: Loop Current mixed layer response to Hurricane Lili (2002). Part I: Observations. *J. Phys. Oceanogr.,* **42,** 400–419, doi:10.1175/JPO-D-11-096.1.

Watts, D. R., K. L. Tracey, and A. I. Friedlander, 1989: Producing accurate maps of the Gulf Stream thermal front using objective analysis. *J. Geophys. Res.,* **94,** 8040–8052, doi:10.1029/JC094iC06p08040.

Yabuki, T., T. Suga, K. Hanawa, K. Matsuoka, H. Kiwada, and T. Watanabe, 2006: Possible source of the Antarctic Bottom Water in the Prydz Bay Region. *J. Oceanogr.,* **62,** 649–655, doi:10.1007/s10872-006-0083-1.

Yoneyama, K., C. Zhang, and C. N. Long, 2013: Tracking pulses of the Madden–Julian oscillation. *Bull. Amer. Meteor. Soc.,* **94,** 1871–1891, doi:10.1175/BAMS-D-12-00157.1.